Fermi National Accelerator Laboratory

FERMILAB-FN-669

RF System Considerations for Muon Collider Proton Driver Synchrotrons

J.E. Griffin

Fermi National Accelerator Laboratory
P.O. Box 500, Batavia, Illinois 60510

June 1998

Operated by Universities Research Association Inc. under Contract No. DE-AC02-76CH03000 with the United States Department of Energy

Disclaimer

Distribution

J. E. Griffin
4-20-1998

RF SYSTEM CONSIDERATIONS FOR MUON COLLIDER PROTON DRIVER SYNCHROTRONS

Introduction

The proton driver synchrotron system presently under consideration for the Fermilab muon collider project is projected to consist of two rings, to be operated in series, at a 15 Hz repetition rate. The first ring, termed the Pre-Booster, will have circumference 158.1 m, one third the circumference of the existing Fermilab Booster. Gated Linac pulses of H^- ions will be injected into pre-set Pre-Booster rf buckets at 1 GeV in such a way as to result in four bunches, each containing 2.5×10^{13} protons with longitudinal emittance ~ 1 eV-s. The captured beam is to be accelerated to T = 3 GeV (cp = 3.825 GeV) in ~33 ms. At the extraction energy, the four bunches are to be injected into matched rf buckets in a 474.2 m ring operating at h = 12, and accelerated at the 15 Hz rate to 16 GeV. The four bunches may be injected into adjacent buckets in the h = 12 ring or possibly into four equally spaced buckets. Prior to extraction at 16 GeV the bunches are to be narrowed, presumably by some rf manipulation, to σ ~ 1 ns. Transition, γ_t, in the first ring is set at 5 and in the second ring at 24.

This exercise is intended to be a feasibility study of the rf problems which may arise in a configuration of high intensity rings as described above. The primary rf problems are expected to be potential well distortion caused by space charge forces, and transient beam loading caused by the very high design current (or more directly, the large charge per bunch). This note describes a sequence of steps that could be used to achieve the operation goals. This is not a complete system design. Instead, it is essentially a search for "show-stoppers", problems for which there appears to be no reasonable solution.

Space Charge Potential Well Distortion

The proposed injection energy for the first (pre-Booster) ring is 1 GeV. At that energy the 4 μC bunches will develop substantial resistive wall decelerating voltage and associated potential well distortion.[1] For reasonably long bunches the potential well distortion can be compensated to first order by increasing the fundamental frequency rf voltage. An iteration program has been

developed for calculating the increase in rf voltage necessary to compensate for the anticipated distortion. That program has been used to develop the rf voltage programs shown in this report.[2] For bunches short with respect to an rf period, such as those anticipated at the end of the acceleration cycle where bunches are intentionally shortened, it will be necessary to incorporate additional techniques to compensate for space charge bunch lengthening forces (below transition). It has been shown that intentional introduction of inductance, with appropriate magnitude and bandwidth, into the vacuum chamber may be used to compensate for these forces.[3] There have been two recent tests of this procedure[4,5], and a third test is proposed for the near future at the BNL AGS. In order to develop bunches with sufficiently small longitudinal emittance following injection into the pre-Booster ring, it is proposed to develop some version of this technique using ferrite of appropriate properties. Also, in order to achieve the desired 1 ns rms bunch length prior to extraction at 16 GeV, it is proposed to employ a version of this technique using FeYtGa microwave ferrite in a controllable way in the h=12 ring.

Transient Beam Loading Potential Well Distortion, Single Bunch Effect

Figure 1 shows an rf cavity-like device consisting of a ceramic gap in a beam pipe which is surrounded by a resistive-inductive reactance. A very short bunch (δ-function) of quasi-relativistic charged particles with total charge q passes through the capacitive gap in a time short with respect to the circuit decay time constant. It will, as it departs, deposit a charge on the capacitor equal and opposite to its wall current image charge. The instantaneous voltage on the capacitor will be q/C and the stored energy will be ½CV^2. The energy deposition must result in some deceleration of the bunch. It has been shown that the net decelerating voltage affecting such a bunch is one-half of the voltage developed on the capacitor.[6] For a gap impedance which is resistive or complex, and/or for non δ function distributions, the one-half rule does not apply exactly.

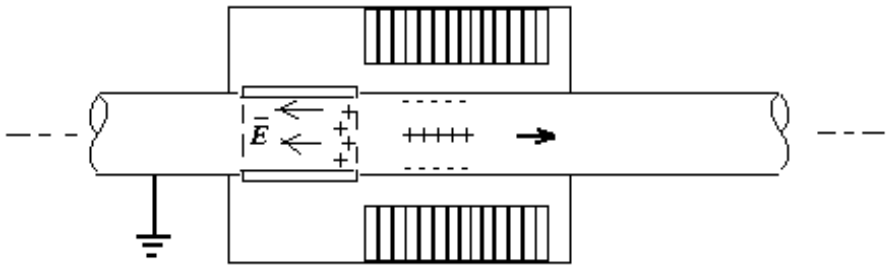

Figure 1. A dielectric gap in a beam pipe surrounded by (or in parallel with) a complex reactance. Proton beam moves to right.

If the line charge distribution has significant length, then a decelerating E field will build as shown during the bunch passage time. The detailed time development of the decelerating field will depend on the bunch shape, the nature of the reactance, and its time constant relative to the total bunch length, cf. Appendix A.

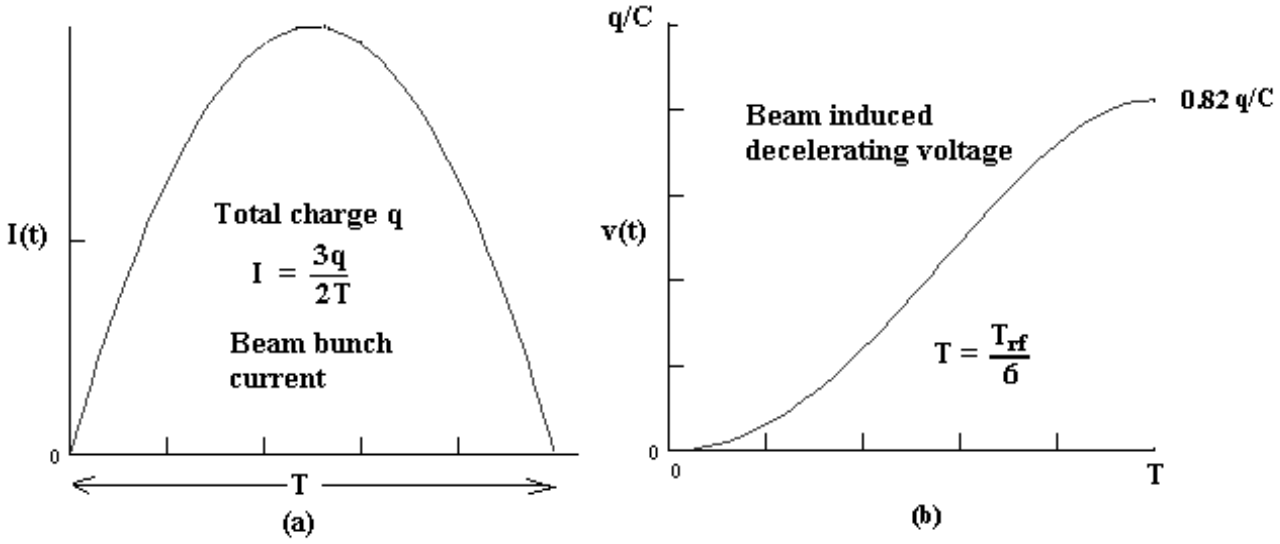

Figure 2. (a) Parabolic line charge distribution, length $T_{rf}/6$ with total charge q.
(b) Decelerating gap voltage on RLC cavity gap with Q = 20.

In Figure 2a, a bunch with total charge q contained within a parabolic line charge distribution with full length T, is shown. In part (b) of the figure the decelerating voltage developed on the gap of an rf cavity is shown as a function of time during the bunch passage. The rf cavity is represented by a parallel RLC circuit assumed to have Q = 20. The bunch length is assumed to be one-sixth of the cavity resonant rf period (~22 ns for the case at hand). It is useful to normalize the transient beam loading voltages to $q/C = V_x$, the maximum voltage a beam bunch can develop on a single pass. In this case the peak voltage developed is 0.82q/C.

With an assumed gap capacitance 500 pF, a 4 μC bunch develops a voltage peak ~6.5 kV in this case. The maximum slope of the transient voltage dv(t)/dt is case ~ 3×10^{11} v/s. The 7.4 MHz cavity, operating at some point in the acceleration cycle at 10 kV with φ_s 45 deg develops an rf focusing slope 4×10^{11} v/s. It is evident that transient beam loading (TBL), voltages may seriously deteriorate or even overpower the effective rf potential well if not compensated for by some technique.

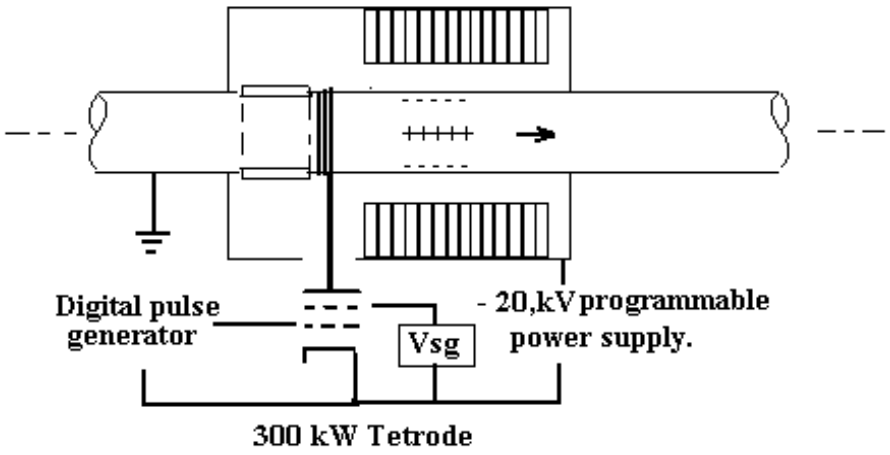

Figure 3. Transient beam loading power tetrode connected directly to an accelerating cavity gap.

Figure 3 shows a large power tetrode with its anode connected directly to an rf cavity accelerating gap. The cathode of the tube is connected to a negative power supply, which is programmable at 15 Hz. The power supply is to be programmed such that it delivers ~2 kV more than the specified rf gap voltage for the rf station. This tube is biased well beyond cutoff so that the quiescent anode current is zero (i.e. the tube is to be operated in "deep class C"). The grid of this tube is to be driven positive just as each beam pulse passes through the accelerating gap. The tube is to deliver just the charge necessary to compensate for the transient beam loading by essentially delivering the electrons necessary for the beam image charge. The grid driving pulse generator is programmed from one or more beam sensing devices so that pulsing occurs at the right time and with correct amplitude regardless of the instantaneous anode voltage, which will vary as a function of the desired anode voltage program. The screen grid voltage on the tube can be varied as a function of the instantaneous anode voltage in such a way that the required grid drive pulse need not be a large function of the anode voltage. (An additional, presumably smaller tube, which excites the cavity with rf power, is operated with a feedback system which always delivers just the power necessary to cause the anode voltage to swing down to about 1 kV above its cathode voltage.) A local 'rf feedback' system can also be installed, using the additional tube, to correct for small errors in the drive amplitude to the compensating tube. It does not appear feasible or necessary to attempt to duplicate exactly the beam pulse shape, as long as the tube delivers the correct charge properly centered on the beam pulse. The driving signal may be a square wave (subject to bandwidth limitations inherent in the tube),

which is delayed a small fraction of the bunch length. Figure 4 is a plot of the cavity response to a 34 ns parabolic bunch and a 29 ns square pulse with equal and opposite charge, and the difference between them. The difference between the beam pulse voltage and that of a properly located rectangular pulse with correct charge is an odd (nearly sinusoidal) function approximately centered on the bunch. This wave shape will make only a minimal disturbance of the rf potential well and a minimal contribution to longitudinal dilution. Also, because the Fourier transform of the difference signal will also be an odd function (of frequency), it will have minimal Fourier current components at the rf frequency or harmonics thereof.

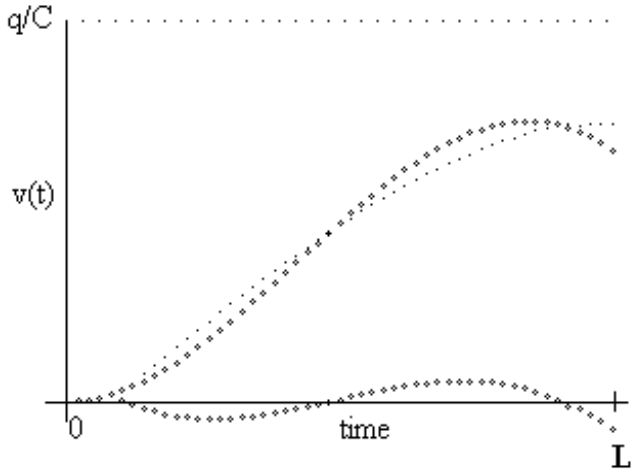

Figure 4. Rf cavity response to a parabolic charge with full width $T_{rf}/4$, a rectangular pulse of the same area, and the difference between them.

Pre-Booster RF Voltage and Bucket Area

The pre-Booster ring will operate at h = 4 over a frequency range 6.639 to 7.37 MHz. During gated linac injection the rf voltage will be varied from 20 kV to 45 kV, at which time each injected bunch, containing 2.5 x 10^{13} protons (4 μC), will have longitudinal emittance ~1 eV-s.[7] The rf system will be designed to develop a minimum of 2 eV-s per bunch during the acceleration cycle. Near the beginning of the cycle additional rf voltage will be required to compensate for bucket area reduction resulting from space charge potential well distortion.[2] In addition to creating bucket area, the rf system must deliver 3.2 x 10^4 J energy to the beam during acceleration. Averaged over the acceleration period, 33 ms, this is ~1 MW. (Averaged over one 15 Hz period, 480 kW.) Figure 5 shows an rf voltage program that will develop a total of 8 eV-s during a sinusoidal acceleration cycle. The accelerating voltage $V\sin\varphi_s$ is proportional d(cp)/dt.

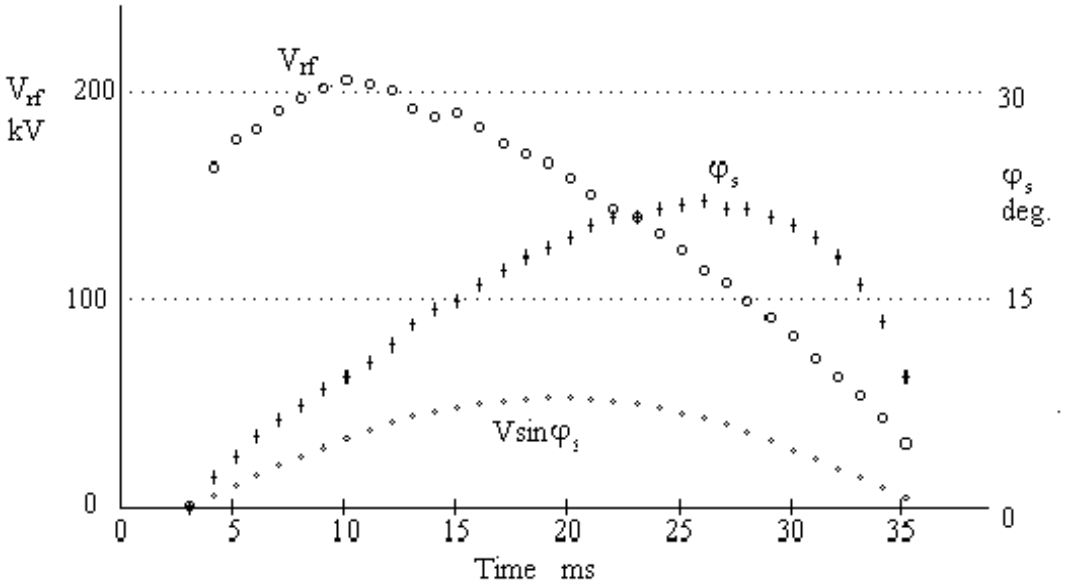

Figure 5. Rf voltage, accelerating voltage $V\sin\varphi_s$, and synchronous phase angle φ_s for constant 8 eV-s bucket area and sinusoidal cp variation.

V_{rf} is the total rf voltage, i.e. the accelerating voltage and the bucket generating voltage. This rf voltage program approaches a very small value near the end of the cycle, where $V\sin\varphi_s$ approaches zero and γ approaches γ_t. (forcing η to approach zero). This is not an acceptable voltage profile for the pre-Booster. The conditions on V and φ_s near the end of the cycle create a long bunch with small momentum spread. The momentum spread cannot be allowed to decrease to such small values without exceeding drastically the threshold for Keil-Schnell instability.[8]

This situation can be ameliorated to some extent by increasing the rf voltage and bucket area during acceleration such that the bunch is narrowed substantially. The extent to which the bunch can be narrowed is limited by the fact that as the bunch becomes narrower the peak current in the bunch increases. The bunch narrowing is limited by the maximum current capability of the feed-forward compensating system. The proposed system should be able to deliver ~170 A pulses.
A parabolic line charge bunch with full width T at the base and containing charge q will have peak current $I_p = 3q/2T$, A 4 μC bunch with peak current 160 A will have full width 37.5 ns (± 50°, in a 7.5 MHz bucket). Such a bunch, with longitudinal emittance 1.1 eV-s, will have energy spread ± 18.7 MeV. The bunch is matched to a 7.5 eV-s bucket with bucket height 44 MeV. This sets the rf voltage at the end of the cycle to ~57 kV. At earlier times in the cycle φ_s must be larger and this will force a reduction in bucket length and matched bunch length.

For given accelerating voltage $V\sin\varphi_s$, larger synchronous phase angles imply larger peak rf voltage, which results in larger anode dissipation in the pulse power tube. The rf voltage throughout the cycle must strike a balance such that the bunch momentum spread remains as high as possible consistent with a limit on the bunch peak current. The shape of the voltage curve can be adjusted by introduction of a small amount of second harmonic on the momentum curve and by passive compensation of space charge potential well distortion.

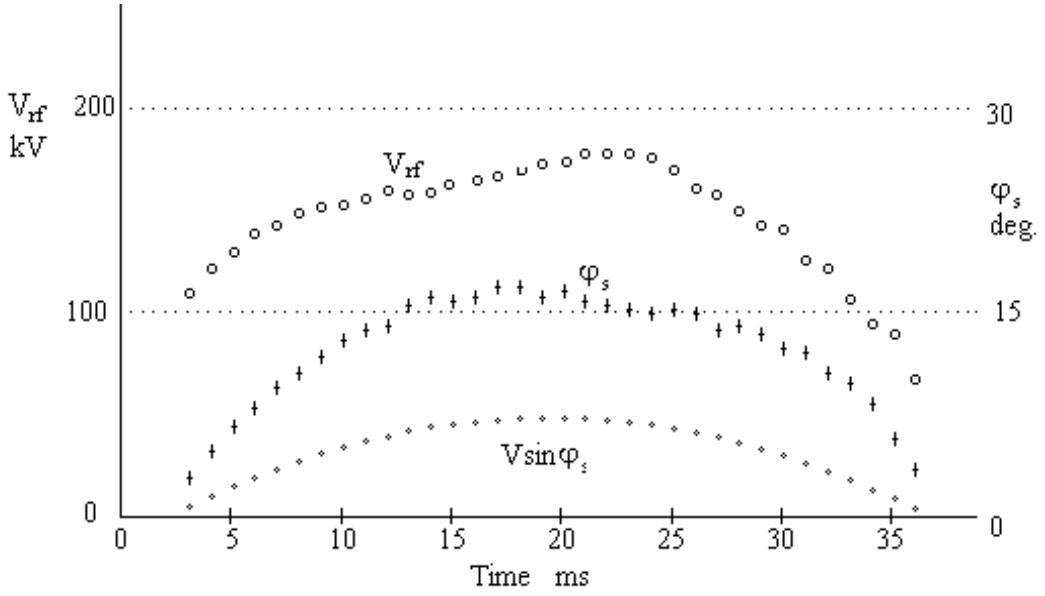

Figure 6. Peak rf voltage, accelerating voltage $V\sin\varphi_s$, and synchronous phase angle φ_s, developing 7.5 to 30 eV-s during acceleration. The guide field has 3.75% second harmonic added and j106 Ω passive space charge compensation is included in the calculation.

Figure 6 is a voltage curve derived by allowing the bucket area to approach 7.5 eV-s quadratically with momentum, while introducing 3.75% second harmonic on the momentum curve and introducing j106 ohms inductive reactance into the vacuum chamber (in addition to a 'normal' inductive Z/n of j20 ohms). The rf voltage reaches a maximum value ~185 kV and φ_s does not exceed ~20 degrees. Using the 'partially filled bucket' curves of Cole and Morton[9] it is shown that the bunch length between 20 and 25 ms on the curve hovers around 45 ns with peak bunch current ~135 A. This voltage curve appears to be a nearly optimum compromise.

RF Cavity Considerations

The 185 kV requirement coupled with the required frequency range might reasonably lead to a choice of ten tunable rf cavities, each developing ~20 kV and capable of delivering 100 kW average beam rf power. This appears to be consistent with straightforward state of the art design. However, the relatively small ring circumference implies the need for rf cavities with larger longitudinal gradient. That concern suggests some slight variations from traditional design.

It may be possible to develop higher voltage gradient cavities through the use of metal alloy (MA), tape wound cores such as Finemet[{10}], Metglas[{11}], or Vitrovac[{12}] in place of NiZn ferrite in the cavities. The alloy cores can sustain roughly a factor of two larger rf B fields (near 7 MHz) than are available in ferrite, but at the cost of dramatically increased power loss. The effective relative permeability, $\mu_{r,}$ of the alloy cores may be substantially larger than that of ferrite, leading to larger inductive reactance for a specified gap voltage. This implies reduced gap capacitance for a given resonant frequency. Capacitance less than 100 pF would typically be required for resonance. If the anodes of either or both of the proposed drive tubes are to be connected directly to the gap, then the output capacitance of the tubes alone would be too large to allow tuning to resonance. Also, the transient beam loading voltages would become unmanageable with reduced gap capacitance (i.e. increased R/Q). Another problem is that the materials are susceptible to large changes in permeability with dc magnetic fields. At 20 cm the H field from the 28 A beam in the pre-Booster will be 22 A/m. This is sufficient to cause a 30% reduction in permeability in 'FT3M' Finemet. Some further investigation is needed.

The gap capacitance, tunability, and R/Q problems may all be resolved by addition to the cavity of one or more 'outboard' inductors. These inductors could take the shape of standard Fermilab tuners, containing NiZn ferrite rings. The added inductors can be provided with bias windings so that the inductance can be changed under program to allow for cavity tuning. The added inductance will store a large fraction of the magnetic energy with the MA (metal alloy) rings providing a large series reactance in small distance. In order to conserve longitudinal space, the outboard inductors may be mounted transversely, diagonally, or even vertically in the enclosure. Figure 7 is a sketch of an rf cavity with metal alloy cores on the beam axis coupled to two power amplifiers and a double ended ferrite inductor containing ferrite cores. The ferrite 'tuner' has bias current windings (probably 8-10 turns) for cavity tuning. One of the power amplifiers is dedicated to transient beam loading compensation while the other delivers cavity rf power. The cavity power amplifier delivers primarily 'bucket area' voltage and rf feedback power.

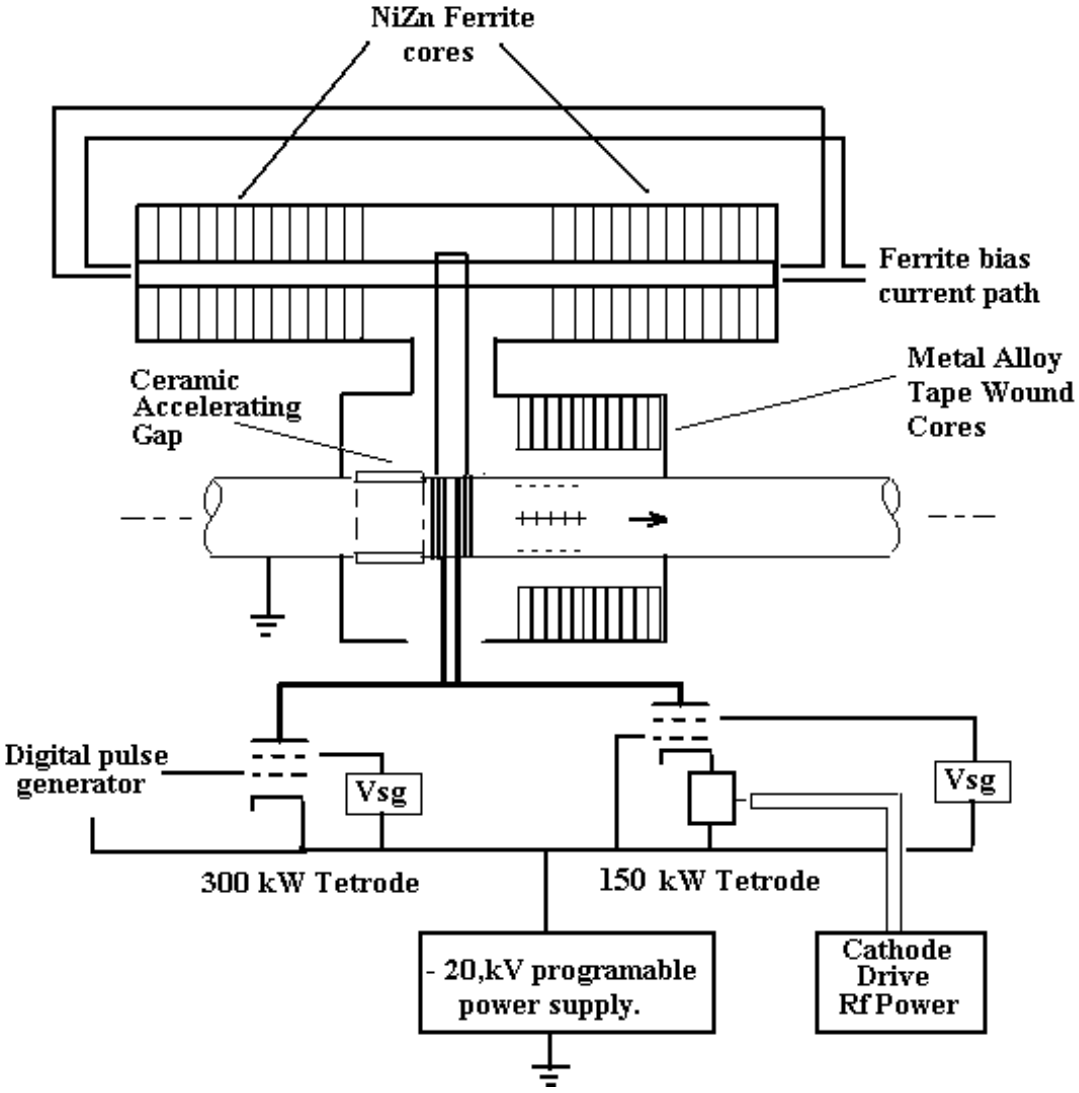

Figure 7. Rf cavity containing metal allow cores on axis and additional ferrite inductance off-axis. Power amplifiers for cavity excitation and transient beam loading compensation are coupled directly to the cavity accelerating gap.

The gap voltage capability of the structure , as proposed, is limited by the rated anode voltage of the power tetrodes and by the voltage hold-off capability designed into the metal alloy rings in the cavity and the ferrite rings in the inductor. A high voltage version of the Eimac 150 kW tube in routine use at Fermilab exists, (Varian Y676A). This tube is rated for use as an rf

amplifier with 35 kV dc anode voltage. Therefore a cavity operating at 30 – 35 kV can be considered.
An ensemble of six or seven 30 kV rf stations might be used to deliver the required ~180 kV pre-Booster voltage requirement. Each of six rf stations would be required to deliver ~167 kW beam power during the acceleration cycle. The ring dc current will be ~28 A during the cycle so that the peak beam power will be $28V\sin\varphi_s \sim 1.4$ MW (233 kW per cavity), near 22 ms.

The geometry shown is single-ended. If inductance were to be placed on either side of the gap, a total single gap voltage ~60 kV could be developed. The cavity would be almost twice as long as the single ended version and the gap voltage would be slightly larger than the 50 kV per gap limit that is frequently allocated to ceramic gaps in an accelerator environment. Also, the proposed transient beam loading compensation scheme works only on the down stream side of a gap because, while a vacuum tube can deliver a burst of electrons to the beam pipe at the gap, it is difficult to remove electrons in this way (unless the gap is connected to the tube cathode, cathode follower style, another approach). The 'aspect ratio' of the MA cavity is adjustable through the choice of the number of cores vs the radial size of each core. The desired reactance may be achieved through the choice of a few large radius cores (i.e. ~ five cores with radius 0.8 m), or a larger number of smaller cores. Because of the physical size of the nearby amplifiers etc. there is little utility in making the cavity 0.1 m long and 1 m across. Probably an optimum geometry would have the length and radial extent nearly equal. Another advantage of the use of MA cores on the beam axis of a cavity system is that the cores need not be circular. In a ring using a high dispersion lattice there may be some space advantage in the use of 'racetrack' shaped cores, with larger horizontal than vertical dimension.

By using data provided by Y. Tanabe, JHF Laboratory[{10}], a rough outline of a cavity design can be developed. At 7 MHz it appears to be useful to split the cores radially and include two 0.5 mm reluctance gaps. With this assumption, the available data indicate Q~3.8 and $\mu_p Qf \sim 1.1 \times 10^{10}$. ($\mu_p$ is the relative permeability which results from measurements interpreted using a parallel RLC circuit to model the material.) The manageable power density is assumed here to be slightly less than the ~ 10 W/cc^3 estimate obtained from Y. Mori, JHP. [{14}]

In order to provide adequate voltage hold-off in the cavity, the inner diameter of the cores is chosen to be 30 cm. The outer diameter is set to be 50 cm and each core width is 2.5 cm. The cores are to be separated by a 1 cm cooling channel. The volume of each core is 3.14×10^4 cm^3 and the flux area 2.5×10^{-3} m^2. The voltage is set at 3 kV per core; ten cores (30 cm including cooling channels), are required. The total cavity length, including gap capacitance, is ~ 50 cm.

Cavity MA core properties;

$\mu_P \sim 414$, Inductance per core ~ 1μH, X_l per core ~ 44 Ω, Shunt resistance R_p per core 167 Ω.

Using ten cores, 3 kV per core, Power per core $P = V^2/2R_p =$ 27 kW or ~ 8.6 W/cm^3.

Total power 270 kW, Total inductive reactance j455 Ω.

With total effective gap capacitance ~500 pF, The capacitive reactance $X_c = X_l = R\backslash Q = 45.5$ Ω. This sets the reactance of the external 'tuning' inductors to j50.6 Ω, or j101 Ω per side, if two back to back inductors are used, as shown. At 7 MHz each inductance will be ~ 2.3 μH.

At maximum V_g the current entering each leg of the tuning inductor will be ~ 297 A. The time averaged stored energy per side will be 0.05 J.

The dimensions of the inductors can be set by allocating a limiting average power density and an appropriate inner radius voltage hold-off dimension. If the power density, averaged over a 15 Hz period, is set at 0.13 W/cc^3, then the power density at the maximum voltage is ~ 0.3 W/cc^3. The inner diameter of the ferrite rings is set at 14 cm.

At 7 MHz, ferrite with unbiased μQf ~ 6 x 10^{10} can be used. With the tuning bias necessary to bring the system to 7 MHz, the ferrite Q will probably exceed 100. Using this value and the stored energy, the peak power dissipated per side will be ~ 22 kW. The required ferrite volume per side is 7.3 x 10^4 cc^3. If the outer diameter of the ferrite rings is chosen to be 36 cm then the effective ferrite length on each side must be 85 cm, or 34 2.5 cm rings per side. The rings may be separated by 5 mm copper cooling washers, bringing the total length of each side to ~ 1.02 m.

The specified inductance of each side, 2.3 μH, can be obtained with this geometry if the relative permeability μ_r at 7 MHz is ~ 14. This is a reasonable value at the relatively high bias value which might be expected near the upper end of the operational frequency range. There should be adequate inductance to tune to the injection frequency, since the unbiased μ_r or the ferrite can be expected to be > 100.

The total energy dissipation in the cavity, exclusive of the anode dissipation of the driver tubes and energy delivered to the beam, will be ~ 320 kW. The time averaged stored energy will be 0.225 J. The 'unloaded' Q at 7 MHz is ~31, with R/Q ~ 45.

If the transient beam loading compensation system were to work perfectly, with the tube exactly matching the beam induced gap voltage at each passage, then presence of beam in the ring would be 'transparent' to the rf cavity. The 'rf' power source would be required to deliver just the energy necessary to develop the required gap voltage at all times during the 50 % duty factor acceleration cycles. The 320 kW peak power requirement appears to within the capability of the proposed 150 kW power tetrode when operated on the 50% duty factor with the proposed rf voltage program (Fig. 6).

The energy delivered to the proton beam by each rf station can be delivered primarily by the transient beam loading power tetrode, connected directly to the accelerating gap by a low inductance conducting strap. The anodes of the two tubes could be located on either side of the rf cavity adjacent to and as close as possible to the ceramic gap. The pulses are to match closely the proton beam pulses in time and total charge, though not necessarily in pulse shape.

In the cavity geometry shown in Fig.7, the rf voltage on the tube anodes is swinging negative with respect to ground during the accelerating phase (this causes an E field directed in the direction of proton motion). The rf voltage curves, Fig.2, show that $V\sin\varphi_s$ is near 48 kV at 20 ms. With six cavities this is 8 kV per cavity. The pulse tube supplies a burst of charge of such a sign that the energy supplied to each beam bunch is $\Delta W = qV\sin\varphi_s = 0.032$ J. These bursts of energy are supplied at the rf frequency rate, 7.4 MHz, so the power delivery at this point in the cycle is 236 kW per cavity, or 1.42 MW. The tube anode voltage at this point will be near (20 kV - $V\sin\varphi_s$), ~15 kV. Because of the relatively high total voltage at this point the instantaneous anode dissipation will be 444 kW. This relatively high dissipation rate results because the tube pulse current is delivered at instantaneous anode voltage $V_{rf}(1 - \sin\varphi_s)$ rather than at the peak of the negative rf swing, as is usually the case in deep class C operation. The instantaneous anode dissipation for the transient compensation tube should be calculated over the entire cycle in order to determine the average dissipation. The 150 kW tube that has been proposed may not be adequate in this configuration. A possible solution to this dissipation problem might be to operate the space charge compensation tubes with a separate programmable cathode power supply, programmed on the $V\sin\varphi_s$ curve rather than on the total anode voltage curve.

H = 12 Booster Ring Rf Voltage and Bucket Area

Near the end of the pre-Booster cycle, the rf voltage is to be raised adiabatically to 57 kV in order to increase the bunch momentum spread. This is done to minimize the possibility of Keil-Schnell instability as γ approaches γ_t. The bunches are finally matched to 7.5 eV-s buckets. Figure 8 is a 2000 particle simulation of a 1.1 eV-s pre-Booster bunch with total bunch length ~37.5 ns and parabolic line charge projection just prior to extraction.

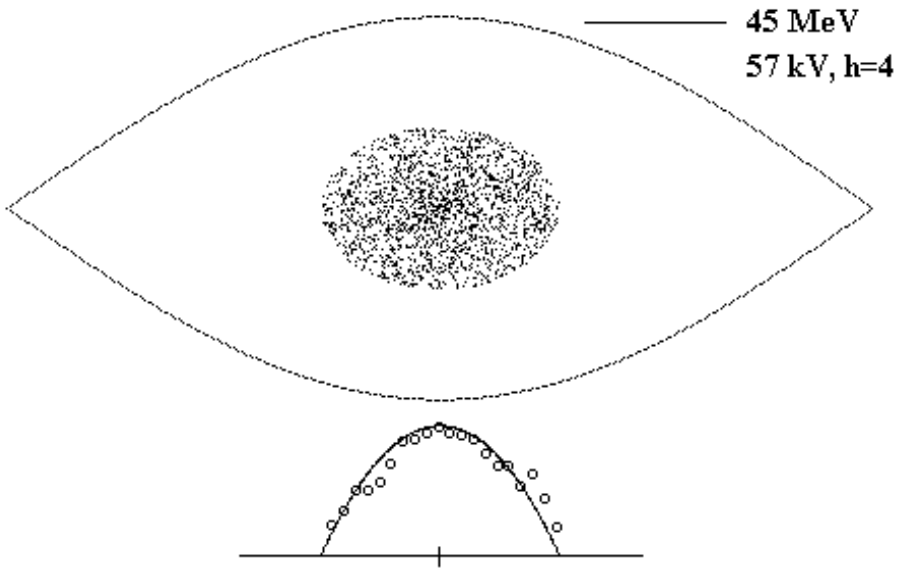

Figure 8. A 1.1 eV-s pre-Booster bunch matched to 7.5 eV-s bucket just at extraction into the Booster.

The pre-Booster bunches are injected into mis-matched 5 eV-s buckets generated by 230 kV in the Booster. In this simulation the rf voltage is held constant for 105 turns (0.17 ms), at the start of acceleration. During this period the injected bunches rotate to ~59 ns full length and $\pm$18.8 MeV energy spread, where they are well matched to a 3.3 eV-s very slightly moving bucket. At that point the rf voltage is dropped to 118 kV and acceleration proceeds with a 3:1 bucket to bunch area ratio. The matched distribution following rotation is shown in Fig 9.

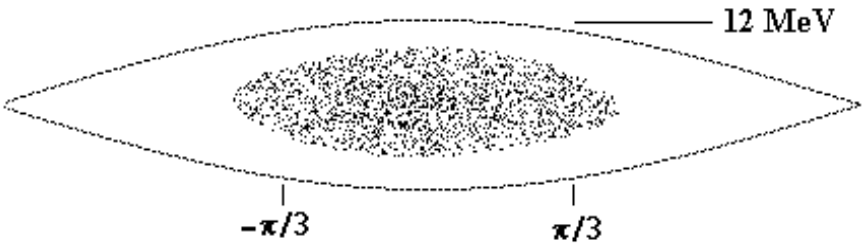

Figure 9. Injected ~1.1 eV-s bunch after 105 turn bunch rotation. The bunch is matched to a 3.3 eV-s bucket generated by 118 kV.

At this point acceleration proceeds with the bucket-to-bunch ratio increasing very slowly until just past the mid-point on the cp(t). As the momentum approaches the maximum value (16.9 GeV/c), the rf voltage is programmed such that the bucket area is increased to 53 eV-s. This is done to prepare the distribution for bunch rotation at the end of the cycle. By introduction of 6% second harmonic on the magnet pc ramp, the rf voltage can be adjusted to remain nearly constant over a large part of the acceleration cycle. A plot of the rf voltage, φ_s, and $V\sin\varphi_s$ is shown in Fig 10.

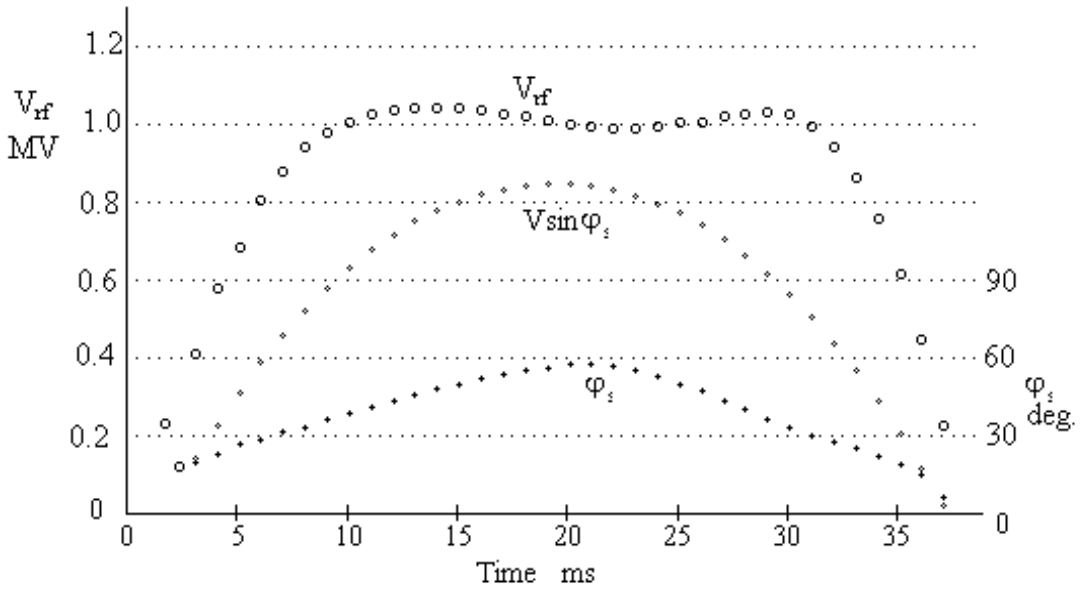

Figure 10. Rf voltage, $V\sin\varphi_s$, and φ_s, during the h=12 Booster cycle. The individual bucket area starts at 3.3 eV-s and ends at 53 eV-s. The guide field ramp has 06% second harmonic component.

Rf Cavities, Power, and Beam Loading

The maximum rf voltage, ~ 1 MV, could be generated by forty of the the tunable composite 30 kV rf cavities described above. Each cavity occupies about 1 m on the beam axis. The physical length of the beam pipe part of the cavity could be shortened by increasing the radial dimension of the metal alloy cores, but the associated power amplifiers and tuning inductors probably cannot be shortened accordingly. Because the h = 12 ring may at some time be required to accept beam directly from a 1 GeV linac rather than the 3 GeV pre-Booster, and because cavity tunability is useful in compensation for steady state beam loading, it seems prudent to retain the tuning capability of the cavities.

The dc current in the ring will reach 9.87 A at maximum intensity (16 μC beam charge). With the proposed pc(t) harmonic content, the maximum value of $V\sin\varphi_s$ is ~850 kV. This sets the peak power delivered to the beam at 8.4 MW, 210 kW per cavity. The average beam power during an acceleration ramp is near 6.5 MW, 162 kW per cavity.

At 20 ms on the ramp φ_s is ~ 58 deg and the total bucket length is ~97 deg. The bunch length at that time will be ~19 ns. If the TBL tube is to deliver 4 μC on this time base the peak current will be 211 A, possibly near the peak current delivery capability. At that point the gap voltage at each cavity will be ~ -22 kV and the energy delivered by the burst of anode current will be 0.088 J. At the rotation frequency this amounts to 52.8 kW, or 211 kW for four bunches, consistent with the above figure. At this point in the cycle the anode voltage on the TBL tube will be ~ $32 - V\sin\varphi_s$ = ~10 kV. The anode dissipation will be ~ 98 kW. This low number is the result of delivery of charge to the beam at a relatively high synchronous phase angle. At other points in the cycle the dissipation will be higher. Nevertheless it may be possible to use 150 kW tubes for TBL, especially if separate programmable cathode power supplies are used for the different types of tubes, as suggested above.

The 'rf' generating tubes, delivering power primarily to excite the cavities (heat up the metal alloy cores essentially), must deliver ~ 320 kW over a large portion of the ramp. If the tubes can be operated near 50% efficiency the anode dissipation, averaged over the 15 Hz machine cycle, may be consistent with the rated 150 kW dissipation of the proposed tubes.

The total rf power delivery capability during the acceleration ramp is estimated to be 30 MW, where pulse power delivery to and from the TBL tubes is included.

Bunch Narrowing Prior to Extraction

In Fig. 11 a charge distribution for a 2 eV-s bunch with $\cos^2$ line charge projection is shown. The bunch is matched to 53 eV-s stationary bucket generated by 165 kV just at the end of the acceleration cycle. The bunch extent is ±68.8 MeV and ±18.5 ns.

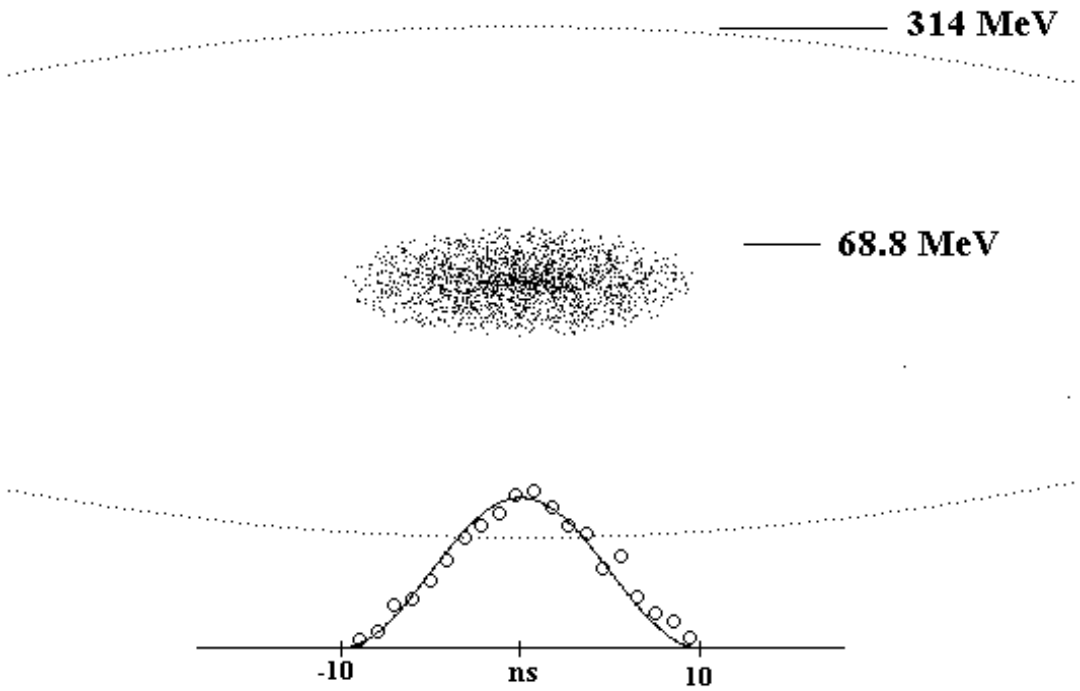

Figure 11. Phase space distribution of 2 eV-s $\cos^2$ line charge bunch, matched to 53 eV-s bucket just prior to bunch rotation at 16 GeV.

Just as the acceleration pc(t) reaches zero slope and the above shown distribution is established, the rf voltage is quickly raised to 1 MV, at the same stationary phase angle. In Fig. 12 the distribution is shown one quarter phase oscillation later, 605 turns. In the simulation no transient beam loading or space charge effects have been included. The result assumes that space charge forces and the effects of transient beam loading have been somehow exactly cancelled. If the 'g_0' factor is 2 then exact cancellation implies that the ring inductance seen by the beam is ~0.6 μH at all Fourier components of the beam distribution. Under these conditions the bunch rotates into a vertical distribution with a sharp peak and full bunch length 7.2 ns. σ is estimated to be ~1.3 ns. Limits representing ±1.2 % momentum aperture are marked. The distribution remains within the labelled aperture limits.

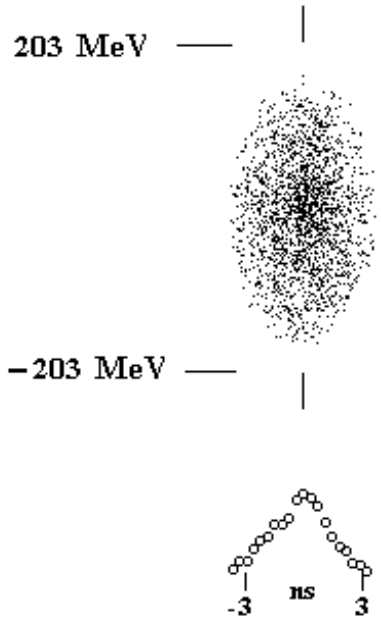

Figure. 12 Distribution after 605 turns. No space charge or transient beam loading effects included in the calculation.

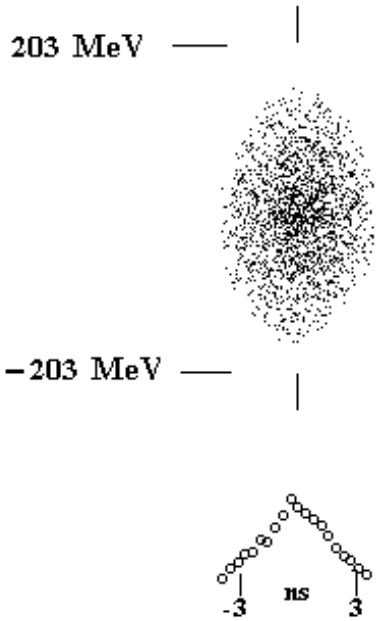

Figure 13. Same distribution with – 1 μH ring inductance included to simulate space charge internal force. Bunch length is 7.7 ns.

The space charge self force on the particles within a bunch, in volts per turn, is proportional to the derivative of the line charge distribution times the effective ring inductance at the Fourier component frequencies within the bunch. For a $\cos^2$ line charge distribution with full length T,

$$I(t) = \frac{2q}{T}\cos^2(\frac{\pi t}{T}), \qquad \frac{dI}{dt} = \frac{2\pi q}{T^2}\sin(\frac{2\pi t}{T}), \qquad \mathrm{V_{sc}\,(t)/turn} = (\mathrm{L/turn})\frac{2\pi q}{T^2}\sin(\frac{2\pi t}{T}).$$

The effective inductance per turn is;

$$L_{eff}/\mathrm{turn} = \frac{1}{\Omega_0}[\frac{g_o Z_o}{2\beta\gamma^2} - L_{ring}], \quad \text{where} \quad g_o = 1 + 2\ln\frac{b}{a} \quad \text{and} \quad Z_o = 377\ \Omega.$$

The effect of space charge can be simulated by introducing a negative value for the ring inductance to reduce the effect of the natural inductance to or below zero. Figure 13 shows a similar distribution (each simulation starts with a different 'random' selection), in which –1.6 μH has been introduced into the (simulated) vacuum chamber. With T = 10 ns and effective ring inductance – 1 μH, the $V_{sc}\sin(2\pi t/T)$ sinusoidal space charge voltage is $V_{sc} \sim$ -240 kV.

In Fig. 14 a similar initial distribution is shown after rotation in which space charge forces have been overcompensated. An additional 3 μH ring inductance has been added so that the space charge voltage is ~ 480sin(2πt/T) kV. Below transition the inductive overcompensation causes spontaneous self bunching. The full bunch width at the base is 6.45 ns and the final momentum spread fits within the designated momentum aperture.

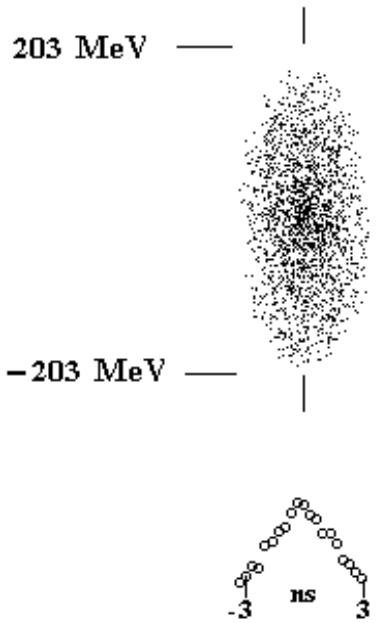

Figure 14. Rotation with 3 μH additional inductance added to the vacuum chamber. Total bunch length 6.45 ns.

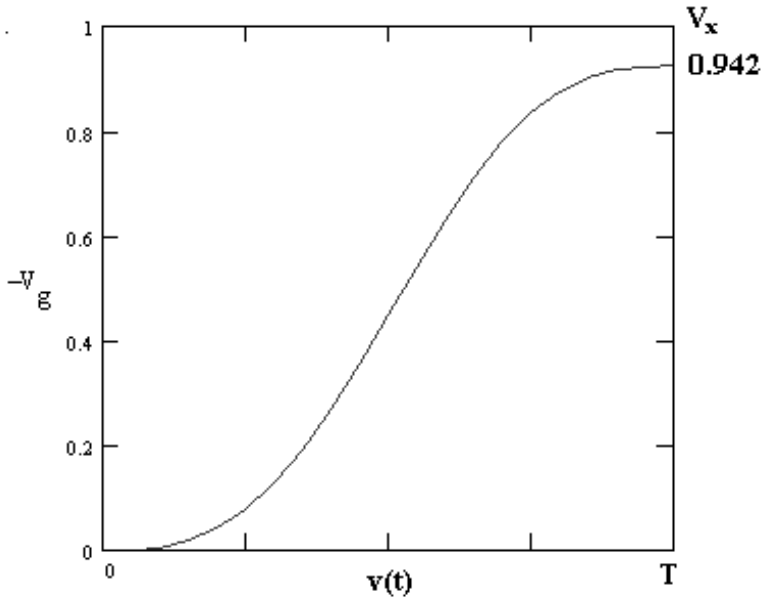

Figure 15. Gap voltage as a function of time for 10 ns bunch ($0.075T_{rf}$) in cavity with Q = 5 and C_g = 500 pf.

The distribution shown in Fig. 14 would approach the specification for final bunch length with σ near 1 ns. Unfortunately, as the bunches are narrowed the peak current increases and the transient beam loading voltage developed on each gap capacitor approaches the maximum value q/C. In Fig. 15 the transient beam loading voltage generated by a $\cos^2$ line charge distribution is shown as a function of time during the bunch, in a cavity with gap capacitance 500 pF and Q=3. The bunch is assumed to be 10 ns full length, i.e. $0.075T_{rf}$. The voltage rises roughly sinusoidally as the bunch passes. The maximum voltage is 0.924q/C = 7.4 kV per cavity. For forty cavities, the maximum voltage is 296 kV. The maximum slope of this waveform as the bunch passes each gap is ~ -9×10^{13} V/s. The maximum slope of the 1 MV rf bunching wave form is 4.7×10^{13} V/s. It is clear that this effect is so large that the effective bunching voltage slope may be reduced to zero and even changed in sign as the bunches become narrow during rotation. In Fig.16 the initial distribution is shown rotated in the presence of 4 μC, 500 pF,

transient beam loading voltage. Because all of the particles in the bunch see a decelerating voltage, the momentum of the entire ensemble is reduced and all particles drift toward later time.

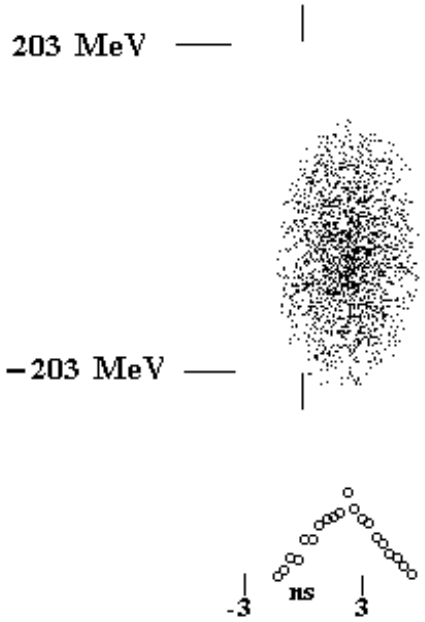

Figure 16. Initial distribution rotated with beam induced voltage transient gap voltage with C_g = 500 pF and Q = 5.

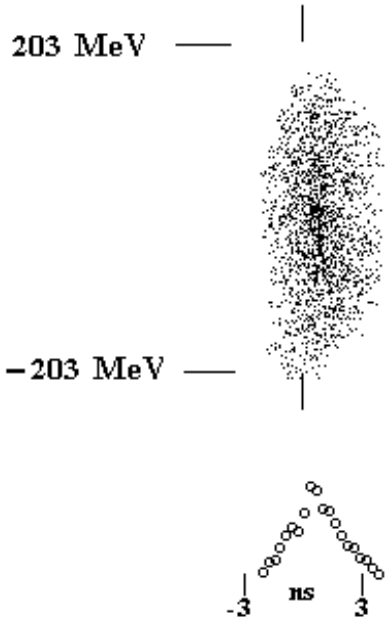

Figure 17. Initial distribution rotated with 100 kV peak transient beam voltage and 5 μH added vacuum chamber inductance. Full bunch length is 6.1 ns.

`

It is evident that transient beam loading (TBL) voltages, if uncompensated, may reduce the slope of the rf wave (as seen by particles within the bunch), to zero or to negative values. It is also true that overcompensation for space charge forces by the intentional introduction of inductance into the vacuum chamber can increase the effective slope of the rf wave, at least near the center of the bunch. Figure 17 is a plot of the result of rotation of the initial distribution in which 100 kV TBL voltage and 5 μH of introduced inductance have been included. The result is a narrowly peaked distribution with full length 6.1 ns, which falls within the designated momentum aperture. The energy loss and drift to later time have been minimized by the inductive voltage component. This distribution can be interpreted to meet the initial specification for bunch σ, i.e. $\sigma \sim 1$ ns.

In the simulation above it has been assumed that a fraction of the transient beam loading voltage has been cancelled by other means. The TBL tube may not have the capability to deliver the large peak current on the ns time scale necessary. However it may be adequate to set the timing

such that the tube delivers a pulse charge equal to the bunch charge, starting slightly in advance of the arrival of the bunches at each gap.

The introduced ferrite must have sufficient bandwidth (up to ~ 1 GHz), to cover the Fourier components of the bunches as they reach their narrowest configuration. This is possible using microwave ferrite such as FeYtGa (YIG) ferrite. However, it will probably be necessary to bias the ferrite near saturation and above its magnetic resonance frequency, at which frequency the ferrite becomes very lossy. In such a bias condition the relative permeability will be reduced to ~ 5, so that, depending somewhat on the core size, the available inductance will be ~ 1 μH /m. Relatively long ferrite insertions may be needed.

Conclusions

A series of design approaches which appear to achieve the specified design goals for rf acceleration and bunch manipulation in the Muon Proton Driver have been presented. The design techniques proposed here are certainly not the only possible approaches. It may be that a final design will be quite different. However, the use of one of the 'new' materials - Finemet, Metglas, or Vitrovac - in conjunction with ferrite appears promising. The benefits of these new materials appears to be in physical size, and in allowing a slightly different approach to the transient beam loading problem. Operational cost and technical difficulties in cooling such systems at very high dissipation levels should be carefully examined. Prototypes of several proposed designs, along with experimental techniques for evaluation of their operation, should be developed as soon as possible.

Acknowledgements

Many people have contributed to the ideas and concepts for a high intensity Proton Driver Synchrotron for the muon collider project during the last year. Too many to mention here. To any left out I express my apology. Salient contributors have been C. Ankenbrandt, K.Y. Ng, Z. Qian, I. Kourbanis, C. Johnstone, M. Popovic, F. Mills, and special thanks to Q Kerns[14].

References

1. S. Hansen, H.G. Hereward, A. Hofmann, K. Hübner, S, Myers, IEEE Trans. Nucl. Sci., NS-22, No.3, 1381, (1975).
2. J.E. Griffin, "Bunches, Buckets, Space Charge, and all that", Mcol. Note., 1-18-'97.
3. A.M. Sessler and V.G. Vaccaro, Passive Compensation of Longitudinal Space Charge Effects in Circular Accelerators: The Helical Insert, CERN, ISR Div. 68-1
4. J.E. Griffin, K.Y. Ng, Z.B. Qian and D. Wildman, Experimental Study of Passive Compensation of Space Charge Potential Well Distortion at the Los Alamos National Laboratory Proton Storage Ring, Fermilab FN-661,(1997).
5. K. Koba, Preliminary Report on Passive Compensation Experiment in KEK PS, presented at JHP Workshop, KEK Tanashi, (3, 1998).
6. P.B. Wilson, PEP–Note 37, SPEAR-163, (1973).
7. I. Kourbanis, private communication, ESME results
8. E. Keil and W. Schnell, CERN Report IST-TH-RF/69-48, (1969).
9. F.T. Cole and P.L. Morton, "Areas and Bunching Factors of Partially Filled Buckets" UCID 10130, (1964). (Copies available from me on request.)
10. Y. Tanabe, Evaluation of Magnetic Alloys for JHF RF Cavity, KEK-JHF JP, (1998).
11. METGLAS, Amorphous Magnetic Materials, Metglas Products, Parsippany N.J,
12. P. Ausset et al, A High Power Multiple Harmonic Acceleration System for Proton- Heavy-Heavy-Ion Synchrotrons, (Dallas Mtg . 1996??)
13. Y. Mori, KEK Tanashi Lab., Private Communication, (March, 1998).
14. Q. Kerns, Introduction to Synchrotron RF Systems for High Bunch Current, Fermilab, (11-1997).